

Bright three-color entangled state produced by cascaded optical parametric oscillatorsAihong Tan,^{1,2,*} Changde Xie,¹ and Kunchi Peng¹¹*State Key Laboratory of Quantum Optics and Quantum Optics Devices, Institute of Opto-Electronics, Shanxi University, Taiyuan 030006, People's Republic of China*²*Laboratory for Quantum Information, China Jiliang University, Hangzhou, Zhejiang 310018, People's Republic of China*

(Received 14 July 2011; published 17 January 2012)

We propose a generation system of continuous-variable (CV) three-color entangled state of bright optical beams based on two cascaded standard nondegenerate optical parametric oscillators (NOPOs) above the threshold. One of signal and idler beams produced by the first NOPO is used for the pump light of the second NOPO. The three-color entanglement among signal and idler beams produced by the second NOPO and the retained another beam of the first NOPO is theoretically demonstrated. The symplectic eigenvalues of the partial transposition covariance matrix of the generated optical entangled state are numerically calculated in terms of experimentally reachable system parameters. The optimal operation conditions of the cascaded NOPOs system for obtaining high entanglement are found. The calculated results explicitly demonstrate that the OPO action can transfer entanglement. Due to that the cavity parameters and the nonlinear crystals of the two NOPOs can be freely chosen, the flexibility of the proposed protocol is relatively good and the system can be also extended to prepare entangled states with more parts easily.

DOI: [10.1103/PhysRevA.85.013819](https://doi.org/10.1103/PhysRevA.85.013819)

PACS number(s): 42.50.Dv, 03.67.Mn, 03.65.Ud, 03.67.Bg

I. INTRODUCTION

A variety of physical systems are currently under investigation to perform the envisioned information tasks, e.g., storage, computation, and communications [1]. These systems, such as atom clouds [2], quantum dots [3], and trapped ions [4], all with different resonance frequencies, will probably be used in nodes of quantum networks. To establish entanglement and transfer quantum information among different nodes in a quantum network, we, first, have to prepare multicolor optical entangled states with required different frequencies [5].

In the achieved most experiments, the entangled optical beams are generated by combining squeezed states of light on optical beam splitters [6–9]. As is well known, a beam splitter only implements the linear optical transformation and does not lead to entanglement of optical field with different frequencies. In order to produce multicolor entangled beams, it is important to explore efficient and feasible nonlinear optical systems.

Although the bipartite entanglement between signal and idler output optical fields from a nondegenerate optical parametric oscillator (NOPO) has been experimentally observed by several groups [10–14], the observation of three-color entanglement is much harder. Recent years, some generation schemes of continuous-variable (CV) multiply entangled beams with different frequencies via intracavity nonlinear optical processes have been proposed [15–21]. Especially, the genuine three-color pump-signal-idler entanglement produced directly from a standard single NOPO above the threshold was theoretically demonstrated in 2006 [15] and experimentally realized at a low temperature of -23°C in 2009 [16].

Based on the existence of the tripartite entanglement among the three optical fields produced by an optical parametric oscillator (OPO) operating above threshold, a scheme to generate CV multicolor entangled state using various OPOs in a chain configuration has been proposed in 2008 [22]. In

the scheme proposed by Cassemiro and Villar, the pump field reflected by the first OPO is used for the pump mode of the second OPO. Since the reflected pump mode is entangled with the signal and the idler modes produced by the first OPO through the frequency down-conversion, the signal and the idler modes generated by the second OPO are also entangled with that produced by the first OPO. A pair of the signal and the idler modes is usually named as a twin beam. In this case, the reflected pump field serves as an entanglement distributor between two OPOs. It has been pointed out in Ref. [22] that “the spurious losses in the pump mode have the main consequence of decreasing the available power for pumping the second OPO.” In 2010, the entangled state of photon triplets was experimentally produced by cascaded spontaneous parametric down-conversion (C-SPDC), in which each of the triplet photons originated from a single pump photon and, thus, they were quantum correlated [23]. Since the generation process of the triplet-entangled photons in this experiment did not involve usually postselecting [24–27] and heralding [28–30] technology, it was suitable to be used for linear optical quantum computing [31]. The wavelengths of the generated triplet photons in the experiment were 848, 1590, and 1510 nm, respectively, two of which were matched for optimal transmission in optical fibers and, thus, were suitable for three-party quantum communication [32].

Combining the mature generation technology of CV two-partite entanglement using NOPO [10–13] and the idea of transferring quantum correlations among different parts of the spectrum of light [22,33–36], we transfer the above-mentioned scheme producing photon triplets to prepare CV three-color entanglement of optical field. In this paper we propose a generation system of CV three-color entangled optical beams, in which two cascaded NOPOs (NOPO1 and NOPO2) are utilized. One of the entangled signal and idler beams output from NOPO1 is used for the pump light of NOPO2. The well phase-matching among the pump, signal, and idler fields in each NOPO results in the quantum correlations of the amplitude and phase quadratures between output signal and

*tanah@cjlu.edu.cn

idler beams. Because the output signal and idler optical fields from NOPO2 and the retained another beam produced by NOPO1 derive from an original pump field of NOPO1, the CV quantum correlations should exist among the three fields. Based on solving the Langevin equations for the evolution of the field fluctuations inside NOPO1 and NOPO2 [37,38] and applying the necessary and sufficient entanglement criterion for Gaussian states based on the positivity under partial transposition (PPT) proposed by Simon and Werner *et al.* [39,40], we theoretically demonstrate that the determinate CV quantum entanglement exists among the three optical modes with different wavelengths produced by the cascaded NOPOs. Since one of the output beams from NOPO1 is used for the pump field of NOPO2, its quantum fluctuations and its quantum correlations with another output beam from NOPO1 will directly be coupled into the signal and the idler modes of NOPO2 through an intracavity nonlinear interaction. Therefore, in the calculation the pump field of NOPO2 cannot be regarded as a coherent state of light as usual but an asymmetric thermal state depending on the squeezing parameter of NOPO1. The generation of the three-color entanglement closely relates to two nonlinear processes happened in both NOPO1 and NOPO2; therefore, the optimal operation conditions and the cavity parameters of the cascaded system have to be comprehensively considered. We search the optimal pump parameters and the transmissivities of the output coupler for the two NOPOs through the numerical calculation to make the smallest symplectic eigenvalues of the partial transposition covariance matrix of the generated three optical fields reaching the minimum first. Then around these optimal values, the dependences of the smallest symplectic eigenvalues of the partial transposition covariance matrix on the system parameters of the two NOPOs are analyzed. All values of the system parameters used in the calculation are taken within the experimentally reachable regions. The calculated results verify the existence of the expected CV three-color entanglement under some reachable conditions. The calculated results explicitly demonstrate that the OPO action can transfer entanglement and we model a typical experimental setup which provides a direct reference for the design of experimental systems. Due to that the cavity parameters and the nonlinear crystals of the two NOPOs can be freely chosen, the system has better flexibility on the choices for physical parameters and wavelengths of the three entangled modes. On the other hand, since OPO is a well-known tunable optical device the two cascaded NOPOs can provide large frequency choosing range which is very necessary for the application in quantum information networks.

The paper is organized as follows. In the second section, the physical system of the cascaded NOPOs is briefly described and the fundamental formulas of the field fluctuation evolution are deduced based on Langevin equation for standard NOPOs. Then the fluctuations of amplitude and phase quadratures of the output signal and idler fields are calculated by using the boundary conditions of NOPOs. Utilizing the PPT criterion for the inseparability of optical fields [39,40], the entanglement characteristics of the three-color entangled optical beams are numerically analyzed in Sec. III. The influences of the excess phase noise due to thermal fluctuations to entanglement are

discussed in Sec. IV. Finally, a brief summary is given in Sec. V.

II. PHYSICAL SYSTEM AND EVOLUTION FORMULAS OF FIELDS

The schematic of the physical system is shown in Fig. 1. The system consists of two cascaded optical parametric oscillators (NOPOs). Each of NOPOs is composed of the input and output optical couplers, between which a type II phase-matched $\chi^{(2)}$ nonlinear crystal is placed. The parametric interaction is enhanced by the feedback of the optical cavity, in which the three intracavity modes of signal, idler, and pump fields resonate simultaneously. $a_{p1}^{in}(a_{p2}^{in})$ is the pump field of NOPO1 (NOPO2) and $a_{0(1)}^{in}(a_{2(3)}^{in})$ is the injected vacuum signal (idler) fields in two polarization directions of the type II crystal, respectively. The output signal light a_0^{out} from NOPO1 is used for the pump field of NOPO2 ($a_{p2}^{in} = a_0^{out}$) and the idler light a_1^{out} from NOPO1 is retained. a_2^{out} and a_3^{out} stand for the output signal and idler beams from NOPO2. Due to the conservation of energy and momentum in the intracavity frequency down-conversion process and the mode-selecting effect of the resonant cavity, the frequencies of the pump, signal, and idler modes (f_{p1}, f_0, f_1 for a_{p1}, a_0, a_1 and f_{p2}, f_2, f_3 for a_{p2}, a_2, a_3 , respectively) have to satisfy the relations of $f_{p1} = f_0 + f_1$ and $f_{p2} = f_2 + f_3$.

The amplitude (\hat{x}) and the phase (\hat{y}) quadrature operators are defined by the field annihilation operator \hat{a} , i.e., $\hat{a} = e^{i\theta}(\hat{x} + i\hat{y})$, where θ is an arbitrary phase. Generally, θ is chosen to make the average value of the imaginary part of \hat{a} to be zero, i.e., $\langle \hat{y} \rangle = 0$. In this case, \hat{x} and \hat{y} are associated with the amplitude and the phase components of an intense optical field, respectively. In the linearized description of field with $\delta\hat{a} = \hat{a} - \langle \hat{a} \rangle$, the field fluctuations are expressed by the vectors \vec{X}_i ($i = 1$ and 2 for NOPO1 and NOPO2, respectively) [41].

$$\vec{X}_1 = [\delta x_{p1}, \delta y_{p1}, \delta x_0, \delta y_0, \delta x_1, \delta y_1]^T, \quad (1)$$

$$\vec{X}_2 = [\delta x_{p2}, \delta y_{p2}, \delta x_2, \delta y_2, \delta x_3, \delta y_3]^T, \quad (2)$$

where $\delta x_{p1}, \delta x_0, \delta x_1$ ($\delta x_{p2}, \delta x_2, \delta x_3$) and $\delta y_{p1}, \delta y_0, \delta y_1$ ($\delta y_{p2}, \delta y_2, \delta y_3$) are the fluctuations of the amplitude and the phase quadratures of the intracavity pump \hat{a}_{p1} (\hat{a}_{p2}), signal \hat{a}_0 (\hat{a}_2), and idler \hat{a}_1 (\hat{a}_3) fields for NOPO1 (NOPO2), respectively.

Using the master equation for the density operator and a quasiprobability representation of the field, we can replace the operators with c numbers to obtain a Fokker-Planck equation [38] and its equivalent description by Langevin equations. Under the linearized approach [37] and perfect phase matching,

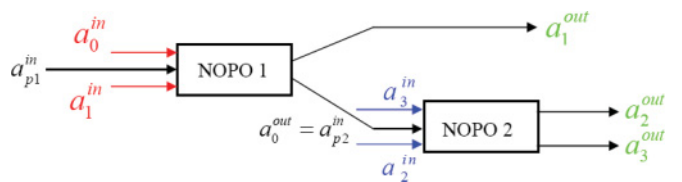


FIG. 1. (Color online) The schematic of physical system for generation of bright three-color entangled state.

the Langevin equations describing the evolution of the field fluctuations inside NOPO1 and NOPO2 are given by

$$\tau_i \frac{\partial}{\partial t} \vec{X}_i = M_{Ai} \vec{X}_i + M_{\gamma i} \vec{X}_{ai}^{\text{in}} + M_{\mu i} \vec{X}_{\beta i}^{\text{in}} + \vec{Q}_i, \quad (3)$$

($i = 1$ for NOPO1, $i = 2$ for NOPO2),

where τ_i is the round-trip time of the optical field inside NOPO_{*i*} and we can take $\tau = \tau_1 = \tau_2$ for all six intracavity fields. M_{Ai} is the drift matrix describing the evolutions of the field fluctuations in a round trip. The next two terms,

$M_{\gamma i} \vec{X}_{ai}^{\text{in}}$ and $M_{\mu i} \vec{X}_{\beta i}^{\text{in}}$, couple the input field fluctuations into the NOPO_{*i*} through its input coupler ($M_{\gamma i}$) and the spurious losses ($M_{\mu i}$). \vec{X}_{ai}^{in} and $\vec{X}_{\beta i}^{\text{in}}$ stand for the fluctuations injected from the input coupler and the noises produced by the internal loss mechanism in NOPO_{*i*}, respectively. \vec{Q}_i expresses the excess phase noise coming from the thermal phonons in the nonlinear crystal.

The drift matrix M_{Ai} , including attenuation, parametric amplification, and phase shift are expressed by M_{A1} for NOPO1 and M_{A2} for NOPO2:

$$M_{A1} = \begin{bmatrix} -\gamma'_{p1} & 0 & -\sqrt{\gamma'_{p1}\gamma'_0(\sigma_1-1)} & 0 & -\sqrt{\gamma'_{p1}\gamma'_1(\sigma_1-1)} & 0 \\ 0 & -\gamma'_{p1} & 0 & -\sqrt{\gamma'_{p1}\gamma'_0(\sigma_1-1)} & 0 & -\sqrt{\gamma'_{p1}\gamma'_1(\sigma_1-1)} \\ \sqrt{\gamma'_{p1}\gamma'_0(\sigma_1-1)} & 0 & -\gamma'_0 & 0 & \sqrt{\gamma'_0\gamma'_1} & 0 \\ 0 & \sqrt{\gamma'_{p1}\gamma'_0(\sigma_1-1)} & 0 & -\gamma'_0 & 0 & -\sqrt{\gamma'_0\gamma'_1} \\ \sqrt{\gamma'_{p1}\gamma'_1(\sigma_1-1)} & 0 & \sqrt{\gamma'_0\gamma'_1} & 0 & -\gamma'_1 & 0 \\ 0 & \sqrt{\gamma'_{p1}\gamma'_1(\sigma_1-1)} & 0 & -\sqrt{\gamma'_0\gamma'_1} & 0 & -\gamma'_1 \end{bmatrix} \quad (4)$$

$$M_{A2} = \begin{bmatrix} -\gamma'_{p2} & 0 & -\sqrt{\gamma'_{p2}\gamma'_2(\sigma_2-1)} & 0 & -\sqrt{\gamma'_{p2}\gamma'_3(\sigma_2-1)} & 0 \\ 0 & -\gamma'_{p2} & 0 & -\sqrt{\gamma'_{p2}\gamma'_2(\sigma_2-1)} & 0 & -\sqrt{\gamma'_{p2}\gamma'_3(\sigma_2-1)} \\ \sqrt{\gamma'_{p2}\gamma'_2(\sigma_2-1)} & 0 & -\gamma'_2 & 0 & \sqrt{\gamma'_2\gamma'_3} & 0 \\ 0 & \sqrt{\gamma'_{p2}\gamma'_2(\sigma_2-1)} & 0 & -\gamma'_2 & 0 & -\sqrt{\gamma'_2\gamma'_3} \\ \sqrt{\gamma'_{p2}\gamma'_3(\sigma_2-1)} & 0 & \sqrt{\gamma'_2\gamma'_3} & 0 & -\gamma'_3 & 0 \\ 0 & \sqrt{\gamma'_{p2}\gamma'_3(\sigma_2-1)} & 0 & -\sqrt{\gamma'_2\gamma'_3} & 0 & -\gamma'_3 \end{bmatrix} \quad (5)$$

where γ_j and μ_j ($j = p1,0,1$ and $p2,2,3$) are associated with the transmission loss (γ_j) of the output coupler of NOPO and all other loss mechanisms (μ_j), respectively. The subscripts $j = p1,0,1$ and $p2,2,3$ designate the pump, signal, and idler fields for NOPO1($p1,0,1$) and NOPO2($p2,2,3$), respectively. γ_j depends on the amplitude reflection coefficients r_j and the transmission coefficients t_j of the output coupler of NOPO by $r_j = 1 - \gamma_j$, $t_j = \sqrt{2\gamma_j}$. μ_j relates to the crystal absorption, surface scattering, imperfection of cavity mirrors of NOPO, and so on. Combining the two loss parameters together, we use $\gamma'_j = \gamma_j + \mu_j$ to denote the total loss coefficient. σ_1 and σ_2 are the pump parameters of the NOPO1 and NOPO2, respectively.

The fluctuation coupling terms $M_{\gamma i}$ and $M_{\mu i}$ are associated with the diffusion in the Langevin process and are described by the diagonal matrices [41]:

$$M_{\gamma 1} = \text{diag}[\sqrt{2\gamma_{p1}}, \sqrt{2\gamma_{p1}}, \sqrt{2\gamma_0}, \sqrt{2\gamma_0}, \sqrt{2\gamma_1}, \sqrt{2\gamma_1}], \quad (6)$$

$$M_{\gamma 2} = \text{diag}[\sqrt{2\gamma_{p2}}, \sqrt{2\gamma_{p2}}, \sqrt{2\gamma_2}, \sqrt{2\gamma_2}, \sqrt{2\gamma_3}, \sqrt{2\gamma_3}],$$

$$M_{\mu 1} = \text{diag}[\sqrt{2\mu_{p1}}, \sqrt{2\mu_{p1}}, \sqrt{2\mu_0}, \sqrt{2\mu_0}, \sqrt{2\mu_1}, \sqrt{2\mu_1}],$$

$$M_{\mu 2} = \text{diag}[\sqrt{2\mu_{p2}}, \sqrt{2\mu_{p2}}, \sqrt{2\mu_2}, \sqrt{2\mu_2}, \sqrt{2\mu_3}, \sqrt{2\mu_3}]. \quad (7)$$

The excess phase noise coming from the thermal phonons in the crystal is a stochastic fluctuation and exists in all intracavity modes. The vector \vec{Q}_i is expressed by

$$\vec{Q}_1 = [0, \delta Q_{p1}, 0, \delta Q_0, 0, \delta Q_1]^T, \quad (8)$$

$$\vec{Q}_2 = [0, \delta Q_{p2}, 0, \delta Q_2, 0, \delta Q_3]^T.$$

In the frequency domain, the intracavity fluctuations of the NOPO1 and NOPO2 are given by Ref. [41]

$$\vec{X}_i(\Omega) = [i\Omega I - M_{Ai}]^{-1} (M_{\gamma i} \vec{X}_{ai}^{\text{in}} + M_{\mu i} \vec{X}_{\beta i}^{\text{in}} + \vec{Q}_i), \quad (9)$$

where the parameter Ω is the analysis frequency. Because we discuss the cascaded nonlinear optical process in two NOPOs, the analysis frequencies for NOPO1 and NOPO2 are taken to be the same in the calculation.

Using the boundary condition on the output coupling mirror [42]

$$\vec{X}_i^{\text{out}}(\Omega) = M_{\gamma_i} \vec{X}_i(\Omega) - \vec{X}_{\alpha_i}^{\text{in}}(\Omega), \quad (10)$$

We obtain the output field of two NOPOs in term of their input fields,

$$\begin{aligned} \vec{X}_i^{\text{out}}(\Omega) &= M_{\gamma_i} [i\Omega I - M_{A_i}]^{-1} (M_{\gamma_i} \vec{X}_{\alpha_i}^{\text{in}} + M_{\mu_i} \vec{X}_{\beta_i}^{\text{in}} + \vec{Q}_i) \\ &\quad - \vec{X}_{\alpha_i}^{\text{in}}(\Omega). \end{aligned} \quad (11)$$

Since $a_0^{\text{out}} = a_{p2}^{\text{in}}$, $\delta x_{p2}^{\text{in}}$, and $\delta y_{p2}^{\text{in}}$ in $\vec{X}_{\alpha_2}^{\text{in}}(\Omega)$ can be replaced by δx_0^{out} and δy_0^{out} in $\vec{X}_1^{\text{out}}(\Omega)$, such that the three designated outputs of the system, δx_1^{out} , δy_1^{out} , δx_2^{out} , δy_2^{out} , and δx_3^{out} , δy_3^{out} are obtained.

III. ENTANGLEMENT CHARACTERISTICS

To verify the quantum entanglement among the obtained three modes, two types of the inseparability criteria for optical modes are used usually. The criterion proposed by van Loock and Furusawa [43] is written directly in terms of the sums of variances involving the following three fields:

$$\begin{aligned} S_1 &= \delta^2(x_1 - x_2) + \delta^2(y_1 + y_2 + g_3 y_3) < 4, \\ S_2 &= \delta^2(x_1 - x_3) + \delta^2(y_1 + g_2 y_2 + y_3) < 4, \\ S_3 &= \delta^2(x_2 - x_3) + \delta^2(g_1 y_1 + y_2 + y_3) < 4. \end{aligned} \quad (12)$$

This is a sufficient condition for the quantum entanglement among amplitude and phase quadratures of three optical modes, i.e., if the three inequalities are simultaneously satisfied, the three modes are in an inseparable entangled state. Where g_i ($i = 1, 2, 3$) are the gain factors (arbitrary real parameters), which are chosen to minimize the combined correlation variances at the left side of the inequalities.

Another criterion based on PPT [39,40] is the sufficient and necessary condition for CV entanglement of Gaussian optical modes. For Gaussian states, the complete information is available from the mean values (first-order moments) and the covariance matrix (second-order moments). As is well known, the second-order moments are relevant for entanglement properties and, thus, the necessary and sufficient entanglement criterion for Gaussian states can be obtained from the covariance matrix, i.e., the PPT criterion [39,40]. If one party is separable from the rest of a multipartite quantum system, the full density matrix remains positive under the partial transposition with respect to that party. The partial transposition for Gaussian state is equivalent to invert the sign of a quadrature of a submode in the state [39]. The state is separable if and only if all the symplectic eigenvalues are greater than or equal to 1. This criterion is necessary and sufficient for all $1 \times N$ decompositions of Gaussian state [40], where $N + 1$ is the total number of entangled modes. In the tripartite scenario, the three possible 1×2 partitions have to be tested.

The covariance matrix of the system is calculated as $V = (\vec{x}^T \vec{x})$, with $\vec{x} = [\delta x_1^{\text{out}}, \delta y_1^{\text{out}}, \delta x_2^{\text{out}}, \delta y_2^{\text{out}}, \delta x_3^{\text{out}}, \delta y_3^{\text{out}}]$. For simplicity and without losing generality, we assume that the losses and transmission factors are the same for signal and idler

modes inside NOPO, i.e., $\mu_0 = \mu_1$ and $\gamma_0 = \gamma_1$ for NOPO1 and $\mu_2 = \mu_3$, $\gamma_2 = \gamma_3$ for NOPO2.

The partial transposition operation may be applied to either a_1^{out} , which results in the partially transposed (PT) covariance matrix $\tilde{V}^{(1)}$, or to one of the twin beams, a_2^{out} and a_3^{out} , which yields $\tilde{V}^{(2)}$ and $\tilde{V}^{(3)}$. The failure of the resultant PT covariance matrix $\tilde{V}^{(i)}$ ($i = 1, 2, 3$) on complying with the uncertainty principle, i.e., $\tilde{V}^{(i)} + i\Lambda \geq 0$, is a sufficient condition for the existence of entanglement between the transposed subset and the remaining subsets [40]. Thus, we can use the smallest symplectic eigenvalue of each PT matrix $\tilde{v}^{(i)}$ for $\tilde{V}^{(i)}$ to witness entanglement, i.e., when $\tilde{v}^{(i)} < 1$ the state is entangled. The symplectic eigenvalues can be computed by diagonalizing the matrix $\Lambda \tilde{V}$, whose eigenvalues turn out to be $\{\mp i \nu_j\}$ for $j = 1, \dots, n$.

Apart from intracavity losses and excess phase noise, which degrade the level of entanglement, there are six system parameters [transmission factors of signal (idler) and pump fields, pump parameters for the two NOPOs], which should be considered comprehensively to achieve the optimal entanglement. We employ in the numerical calculation the analysis frequency $\Omega = 0.01$ and the experimentally reachable system parameters. When $\gamma_1 = 0.03$, $\gamma_{p1} = 0.20$, $\gamma_2 = 0.10$, $\gamma_{p2} = 0.20$, $\sigma_1 \sim 1$, $\sigma_2 \sim 2.02$, the smallest symplectic eigenvalue of $\tilde{V}^{(1)}$ arrives the minimum value $\tilde{v}^{(1)} \sim 0.12$. And when $\gamma_1 = 0.03$, $\gamma_{p1} = 0.20$, $\gamma_2 = 0.10$, $\gamma_{p2} = 0.20$, $\sigma_1 \sim 1$, $\sigma_2 \sim 1$, the smallest symplectic eigenvalue of $\tilde{V}^{(2)}$ and $\tilde{V}^{(3)}$ tends to zero [$\tilde{v}^{(2)}(\tilde{v}^{(3)}) \sim 0$]. Due to the interchangeability of signal and idler modes, we have $\tilde{v}^{(2)} = \tilde{v}^{(3)}$. The results show that the optimal squeezing condition for NOPO1 is near the threshold ($\sigma \sim 1$), which is the same with that for a standard NOPO to achieve the best quantum correlations between output signal and idler modes [37]. The functions of $\tilde{v}^{(1)}$ and $\tilde{v}^{(2)}(\tilde{v}^{(3)})$ versus σ_2 are shown in Fig. 2. We can see that when $\tilde{v}^{(1)}$ reaches to the minimum at $\sigma_2 = 2.02$, $\tilde{v}^{(2)}(\tilde{v}^{(3)})$ is not at the minimum. However, $\tilde{v}^{(2)}(\tilde{v}^{(3)})$ is always smaller than $\tilde{v}^{(1)}$ for any value of σ_2 . To make the balance of $\tilde{v}^{(1)}$ and

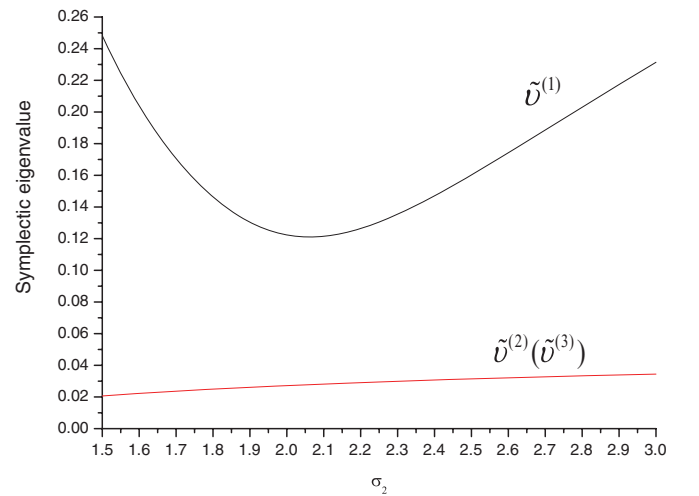


FIG. 2. (Color online) The smallest symplectic eigenvalues $\tilde{v}^{(1)}$ and $\tilde{v}^{(2)}(\tilde{v}^{(3)})$ versus the pump parameter of NOPO2 (σ_2) with $\sigma_1 = 1$, $\gamma'_1 = 0.03$, $\gamma'_2 = 0.10$, $\gamma'_{p1} = 0.20$, $\gamma'_{p2} = 0.20$, $\Omega = 0.01$ [without considering the intracavity losses ($\mu = 0$) and excess phase noise coming from the phonons ($V_Q = 0$) in the crystal].

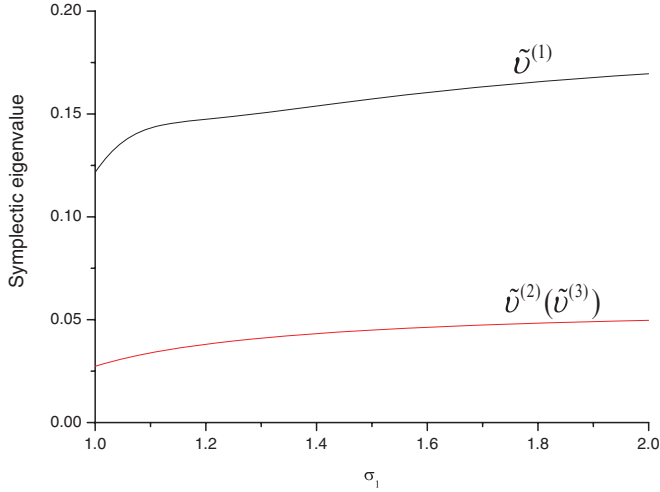


FIG. 3. (Color online) The smallest symplectic eigenvalues $\tilde{v}^{(1)}$ and $\tilde{v}^{(2)}(\tilde{v}^{(3)})$ versus the pump parameter of NOPO1 (σ_1) with $\sigma_2 = 2.02$, $\gamma'_1 = 0.03$, $\gamma'_2 = 0.10$, $\gamma'_{p1} = 0.20$, $\gamma'_{p2} = 0.20$, $\Omega = 0.01$, $\mu = 0$, $V_Q = 0$.

$\tilde{v}^{(2)}(\tilde{v}^{(3)})$ to a large extent, we take $\sigma_2 = 2.02$ in the following calculations.

Figure 3 shows the functions of $\tilde{v}^{(1)}$ and $\tilde{v}^{(2)}(\tilde{v}^{(3)})$ versus the pump parameter σ_1 of NOPO1 under $\sigma_2 = 2.02$ and without considering the intracavity losses ($\mu = 0$) and the excess phase noise ($V_Q = 0$) in the crystal. As that expected for a standard NOPO [37], all $\tilde{v}^{(1\sim 3)}$ tend to the minimum at the pump threshold of NOPO1 ($\sigma_1 = 1$).

The dependences of $\tilde{v}^{(1)}$ and $\tilde{v}^{(2)}(\tilde{v}^{(3)})$ on the transmissions of the signal (idler) mode for NOPO1 ($\gamma_1 = \gamma_0$) and NOPO2 ($\gamma_2 = \gamma_3$) are drawn in Figs. 4(a) and 4(b), respectively, where $\sigma_1 = 1$, $\sigma_2 = 2.02$, $\mu = 0$, $V_Q = 0$ are assumed. The figures show that in a large range of γ_1 ($0.01 \sim 0.10$) and γ_2 ($0.02 \sim 0.15$), the criterion for the entanglement are satisfied, i.e., $\tilde{v}^{(1)} < 1$ and $\tilde{v}^{(2)}(\tilde{v}^{(3)}) < 1$.

Now we consider the effect of the intracavity losses. Figure 5 shows the functions of $\tilde{v}^{(1)}$ and $\tilde{v}^{(2)}(\tilde{v}^{(3)})$ versus μ_1 and μ_2 , respectively, where we have taken $\mu_{p1} = \mu_{p2} = 0.01$ and $V_Q = 0$. The values of $\tilde{v}^{(1)}$ and $\tilde{v}^{(2)}(\tilde{v}^{(3)})$ for $\mu_1 = 0$ are always smaller than that for $\mu_2 = 0$, which means that the influence of the intracavity losses of NOPO1 is stronger than that of NOPO2.

From Figs. 2 to 5, we can see that the values of $\tilde{v}^{(2)}(\tilde{v}^{(3)})$ are totally smaller than that of $\tilde{v}^{(1)}$.

IV. THE EFFECT OF EXTRA PHASE NOISE

It has been pointed out by Cesar *et al.* that there is an additional phase noise source in NOPO above the threshold, which results from the refractive index fluctuation associated with acoustic phonons inside the nonlinear crystal [41]. According to the theoretical model in Ref. [41], we analyze the influence of the extra phase noise from thermal fluctuations in the crystal on the three-color entanglement. The extra phase noise depends on the covariance matrix for the additional phase fluctuations, $V_Q(\Omega) = \vec{Q}(\Omega)\vec{Q}^T(-\Omega)$, in which the covariance terms of the extra noise are given by $\langle \delta Q_j(\Omega)\delta Q_k(-\Omega) \rangle = \eta_{jk}\sqrt{P_j P_k}$, η_{jk} is the noise coupling

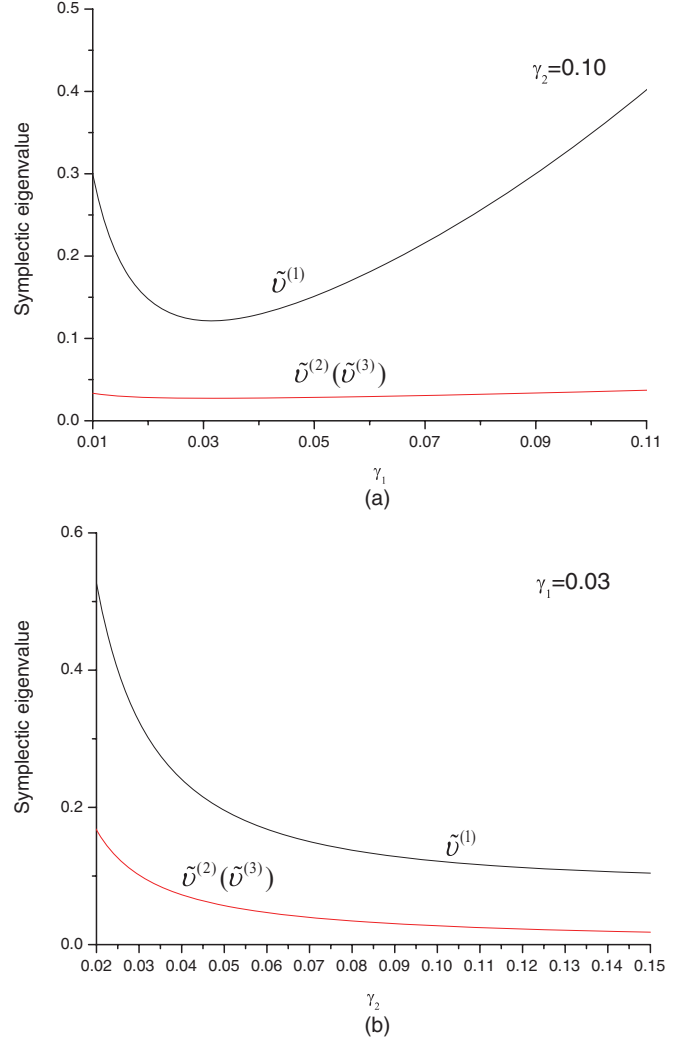


FIG. 4. (Color online) The smallest symplectic eigenvalues $\tilde{v}^{(1)}$ and $\tilde{v}^{(2)}(\tilde{v}^{(3)})$ versus the transmission coefficient of the signal and idler field of the two NOPO with $\sigma_1 = 1$, $\sigma_2 = 2.02$, $\gamma'_{p1} = 0.20$, $\gamma'_{p2} = 0.20$, $\Omega = 0.01$, $\mu = 0$, $V_Q = 0$.

term which depends on the wavelength and the ratio of the crystal length with the effective Rayleigh length of the optical cavity. The extra phase noise is proportional to the square root of the intracavity powers of the optical modes, $\sqrt{P_j}$ and $\sqrt{P_k}$. Based on the analyses in Ref. [41], we assume $\eta_{11} = \eta_{22} = \eta_{00}/4$, $\eta_{01} = \eta_{02} = 0.27\eta_{00}$, and $\eta_{12} = 0.16\eta_{00}$. The value of η_{00} depends on the experiment condition.

The power of the signal, idler, and pump fields for NOPO1 and NOPO2 can be calculated with the Langevin equation [37]. We have

$$|\bar{\alpha}_{p1}|^2 = \frac{\gamma'_0 \gamma'_1}{4\chi_1^2}, \quad |\bar{\alpha}_{p2}|^2 = \frac{\gamma'_2 \gamma'_3}{4\chi_2^2} \quad (13a)$$

$$\begin{aligned} \gamma'_0 |\bar{\alpha}_0|^2 &= \gamma'_1 |\bar{\alpha}_1|^2 = \frac{\gamma'_{p1} \gamma'_0 \gamma'_1}{4\chi_1^2} \left(2\sqrt{\frac{2\gamma_{p1} \chi_1^2}{\gamma'_0 \gamma'_1 \gamma_{p1}^2}} \bar{\alpha}_{p1}^{\text{in}} - 1 \right) \\ &= \frac{\gamma'_{p1} \gamma'_0 \gamma'_1}{4\chi_1^2} (\sigma_1 - 1), \end{aligned} \quad (13b)$$

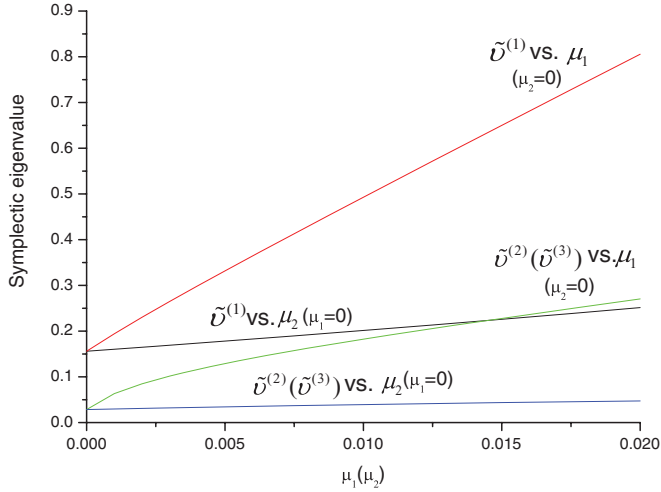


FIG. 5. (Color online) The smallest symplectic eigenvalues $\tilde{v}^{(1)}$ and $\tilde{v}^{(2)}$ ($\tilde{v}^{(3)}$) versus the intracavity losses of the signal and idler field (μ_1 and μ_2) with $\sigma_1 = 1$, $\sigma_2 = 2.02$, $\gamma'_1 = 0.03$, $\gamma'_2 = 0.10$, $\gamma'_{p1} = 0.20$, $\gamma'_{p2} = 0.20$, $\Omega = 0.01$, $\mu_{p1} = \mu_{p2} = 0.01$, $V_Q = 0$.

$$\begin{aligned} \gamma'_2 |\bar{\alpha}_2|^2 = \gamma'_3 |\bar{\alpha}_3|^2 &= \frac{\gamma'_{p2} \gamma'_2 \gamma'_3}{4\chi_2^2} \left(2\sqrt{\frac{2\gamma_{p2} \chi_2^2}{\gamma'_2 \gamma'_3 \gamma'_{p2}} \bar{\alpha}_{p2}^{\text{in}} - 1} \right) \\ &= \frac{\gamma'_{p2} \gamma'_2 \gamma'_3}{4\chi_2^2} (\sigma_2 - 1), \end{aligned} \quad (13c)$$

where χ_1 and χ_2 are the second-order nonlinear coefficients of the type II nonlinear crystals in the NOPO1 and NOPO2, respectively.

If the output power of the signal (idler) field from NOPO1 (assuming that the power of the signal and the idler field is the same) and the oscillation threshold of NOPO2 are given, we can calculate the intracavity powers of signal, idler, and pump fields in NOPO1 and NOPO2 from Eq. (13) and the input-output formulas of NOPO, respectively. Of course, the given output power of the signal field from NOPO1 should be higher than the threshold pump power of NOPO2, otherwise the system cannot be operated.

As an example, we take the really experimental parameters described in Ref. [11] to be that of NOPO1, i.e., $\gamma_1 = 0.016$, $\mu_1 = 0.003$, $\gamma'_{p1} = 0.09$, and $\sigma_1 = 1.9$, where the obtained output power of the signal field is 11 mW (22 mW/2). We assume that it is higher than the threshold of NOPO2. The calculated intracavity powers of the signal and pump fields for NOPO1 are about 345 and 73 mW, respectively. η_{00} is taken as $0.68 \times 10^{-2} \text{ W}^{-1}$ which is the value deduced in Ref. [41] according to the experimental result of Ref. [11].

For reducing the threshold, we choose a periodically poled lithium niobate (PPLN) crystal to be the nonlinear material in NOPO2. For this type of NOPO, the threshold of 1 mW at $1.064 \mu\text{m}$ pump wavelength has been realized [44]. From Ref. [41], we take $\eta_{00} = 0.24 \text{ W}^{-1}$ [41] for NOPO2. If the threshold of NOPO2 (P_2) is 5 mW, the calculated

intracavity powers of the signal (idler) and the pump fields are about

$$|\alpha_2|^2 = |\alpha_3|^2 = \frac{2P_2 \gamma_{p2}}{\gamma'_{p2} \gamma'_2} (\sigma_2 - 1) \sim 97 \text{ mW}, \quad (14)$$

$$|\alpha_{p2}|^2 = \frac{\gamma'_2 |\alpha_2|^2}{\gamma'_{p2} (\sigma_2 - 1)} \sim 47 \text{ mW}. \quad (15)$$

where $P_2 = 5 \text{ mW}$, $\gamma_{p2} = 0.19$, $\gamma'_{p2} = 0.20$, $\gamma'_2 = 0.10$, and $\sigma_2 = 2.02$.

After considering the effect of the excess phase noise coming from the phonons in the crystal, the calculated $\tilde{v}^{(1)}$ and $\tilde{v}^{(2)}$ ($\tilde{v}^{(3)}$) are about 0.56 and 0.18, respectively, both of which are smaller than 1, i.e., the obtained three modes are in a fully inseparable entangled state.

V. CONCLUSION

We design a generation system of CV three-color entangled state in which two cascaded NOPOs are used. The tripartite entanglement at the wavelengths around the optical fiber communication window ($\sim 1.5 \mu\text{m}$) and the atomic transition ($\sim 0.8 \mu\text{m}$) has been experimentally achieved [23]. Using the presented design and the nonlinear crystals utilized in Ref. [23], the CV three-color entanglement of optical field at these wavelengths can be realized. Based on the PPT criterion for the inseparability of three optical modes, the dependences of the symplectic eigenvalues of the partial transposition covariance matrix on the system parameters are calculated. In the calculation, we comprehensively consider the interconnection among the physical parameters of the two NOPOs and find the optimal operation conditions for obtaining better three-color entanglement. Finally, an example associated with the realized experiment shows that the system is able to produce the three-color entangled optical beams. The presented system can be extended to prepare the entangled states with more than three parties if the reflected pump fields are involved or more NOPOs are cascaded. For example, if the two reflected pump fields from the NOPO1 and NOPO2 are involved, as that demonstrated in Refs. [16,22], the entanglement may be generated among five beams with very different frequencies under a suitable condition. In the presented paper, only the optimal conditions for the entanglement of the three transmitted field are considered. For the generation of the entanglement with more submodes the more complex numerical calculations based on the covariance matrix are required. The proposed protocol extends the concept presented in Ref. [16] for the tripartite entanglement generation from a single NOPO to the system of the cascaded NOPOs. Recently, two cascaded OPOs operating below the threshold have been successfully used for the manipulation of a squeezed vacuum and a two-mode entangled state [45,46]. The chaining technique of two OPOs applied in Refs. [45] and [46] can be easily transferred into the proposed protocol. We believe that by combining our proposal and schemes in Refs. [16,22], the multipartite entangled optical states more than three colors can be experimentally achieved.

ACKNOWLEDGMENTS

A.T. thanks X. Jia for the helpful discussion. This research was supported in part by the National Natural Science Foundation of China (Grants No. 61078010 and No. 60736040),

the NSFC project for Excellent Research Team (Grant No. 60821004), and the National Basic Research Program of China (Grant No. 2011CB923103) by the State Key Laboratory of Quantum Optics and Quantum Optics Devices (Grant No. 0901).

-
- [1] M. A. Nielsen and I. L. Chuang, *Quantum Computation and Quantum Information* (Cambridge University Press, Cambridge, 2000).
- [2] C. W. Chou, H. de Riedmatten, D. Felinto, S. V. Polyakov, S. J. van Enk, and H. J. Kimble, *Nature (London)* **438**, 828 (2005).
- [3] M. Atature, J. Dreiser, A. Badolato, A. Högele, K. Karrai, and A. Imamoglu, *Science* **312**, 551 (2006).
- [4] D. Leibfried *et al.*, *Nature (London)* **438**, 639 (2005).
- [5] H. J. Kimble, *Nature* **453**, 1023 (2008).
- [6] X. Su, A. Tan, X. Jia, J. Zhang, C. Xie, and K. Peng, *Phys. Rev. Lett.* **98**, 070502 (2007).
- [7] A. Furusawa, J. L. Sørensen, S. L. Braunstein, C. A. Fuchs, H. J. Kimble, and E. S. Polzik, *Science* **282**, 706 (1998).
- [8] A. Tan, Y. Wang, X. Jin, X. Su, X. Jia, J. Zhang, C. Xie, and K. C. Peng, *Phys. Rev. A* **78**, 013828 (2008).
- [9] M. Yukawa, R. Ukai, P. van Loock, and A. Furusawa, *Phys. Rev. A*, **78**, 012301 (2008).
- [10] A. S. Villar, L. S. Cruz, K. N. Cassemiro, M. Martinelli, and P. Nussenzveig, *Phys. Rev. Lett.* **95**, 243603 (2005).
- [11] X. L. Su, A. Tan, X. Jia, Q. Pan, C. Xie, and P. C. Peng, *Opt. Lett.* **31**, 1133 (2006).
- [12] J. Jing, S. Feng, R. Bloomer, and O. Pfister, *Phys. Rev. A* **74**, 041804(R) (2006).
- [13] A. S. Villar, M. Martinelli, and P. Nussenzveig, *Opt. Commun.* **242**, 551 (2004).
- [14] K. N. Cassemiro *et al.*, *Opt. Express* **15**, 18236 (2007).
- [15] A. S. Villar, M. Martinelli, C. Fabre, and P. Nussenzveig, *Phys. Rev. Lett.* **97**, 140504 (2006).
- [16] A. S. Coelho *et al.*, *science* **326**, 823 (2009).
- [17] S. Zhai, R. Yang, D. Fan, J. Guo, K. Liu, J. Zhang, and J. Gao, *Phys. Rev. A* **78**, 014302 (2008).
- [18] J. Guo, H. Zou, Z. Zhai, J. Zhang, and J. Gao, *Phys. Rev. A* **71**, 034305 (2005).
- [19] S. L. W. Midgley, A. S. Bradley, O. Pfister, and M. K. Olsen, *Phys. Rev. A* **81**, 063834 (2010).
- [20] H. Y. Leng, J. F. Wang, Y. B. Yu, X. Q. Yu, P. Xu, Z. D. Xie, J. S. Zhao, and S. N. Zhu, *Phys. Rev. A* **79**, 032337 (2009).
- [21] H. T. Tan, G. X. Li, and S. Y. Zhu, *Phys. Rev. A* **75**, 063815 (2007).
- [22] K. N. Cassemiro and A. S. Villar, *Phys. Rev. A* **77**, 022311 (2008).
- [23] H. Hubel, D. R. Hame, A. Fedrizzi, S. Ramelow, K. J. Resch, and T. Jennewein, *Nature* **466**, 601 (2010).
- [24] Z. Zhao, Y. Chen, A. Zhang, T. Yang, H. J. Briegel, and J. W. Pan, *Nature* **430**, 54 (2004).
- [25] P. Walther, K. J. Resch, T. Rudolph, E. Schenck, H. Weinfurter, V. Vedral, M. Aspelmeyer, and A. Zeilinger, *Nature* **434**, 169 (2005).
- [26] C. Y. Lu, X. Q. Zhou, O. Guhne, W. B. Gao, J. Zhang, Z. S. Yuan, A. Goebel, T. Yang, and J. W. Pan, *Nat. Phys.* **3**, 91 (2007).
- [27] X. Yao, T. Wang, P. Xu, H. Lu, G. Pan, X. Bao, C. Peng, C. Lu, Y. Chen, and J. W. Pan, e-print [arXiv:1105.6318](https://arxiv.org/abs/1105.6318).
- [28] P. Walther, M. Aspelmeyer, and A. Zeilinger, *Phys. Rev. A* **75**, 012313 (2007).
- [29] S. Barz, G. Cronenberg, A. Zeilinger, and P. Walther, *Nat. Photon.* **4**, 553 (2010).
- [30] C. Wagenknecht, C. Li, A. Reingruber, X. Bao, A. Goebel, Y. Chen, Q. Zhang, K. Chen, and J. W. Pan, *Nat. Photon.* **4**, 549 (2010).
- [31] D. E. Browne and T. Rudolph, *Phys. Rev. Lett.* **95**, 010501 (2005).
- [32] M. Hillery, V. Buzek, and A. Berthiaume, *Phys. Rev. A* **59**, 1829 (1999).
- [33] S. Tanzilli, W. Tittel, M. Halder, O. Alibart, P. Baldi, N. Gisin, and H. Zbinden, *Nature(London)* **437**, 116 (2005).
- [34] P. Kumar, *Opt. Lett.* **15**, 1476 (1990).
- [35] J. M. Huang and P. Kumar, *Phys. Rev. Lett.* **68**, 2153 (1992).
- [36] A. Tan, X. Jia, and C. Xie, *Phys. Rev. A* **73**, 033817 (2006).
- [37] C. Fabre, E. Giacobino, A. Heidmann, and S. Raynaud, *J. Phys. (France)* **50**, 1209 (1989).
- [38] D. F. Walls and G. J. Miburn, *Quantum Opt.* (Springer, New York, 2008).
- [39] R. Simon, *Phys. Rev. Lett.* **84**, 2726 (2000).
- [40] R. F. Werner and M. M. Wolf, *Phys. Rev. Lett.* **86**, 3658 (2001).
- [41] J. E. S. Cesar, A. S. Coelho, K. N. Cassemiro, A. S. Villar, M. Lassen, P. Nussenzveig, and M. Martinelli, *Phys. Rev. A* **79**, 063816 (2009).
- [42] M. J. Collett and C. W. Gardiner, *Phys. Rev. A* **30**, 1386 (1984).
- [43] P. van Loock and A. Furusawa, *Phys. Rev. A* **67**, 052315 (2003).
- [44] M. Martinelli, K. S. Zhang, T. Coudreau, A. Maitre, and C. Fabre, *J. Opt. A: Pure Appl. Opt.* **3**, 300 (2001).
- [45] J. Zhang, C. Ye, F. Gao, and M. Xiao, *Phys. Rev. Lett.* **101**, 233602 (2008).
- [46] Y. Shang, X. Jia, Y. Shen, C. Xie, and K. Peng, *Opt. Lett.* **35**, 853 (2010).